JOURNAL OF PROPULSION AND POWER
Vol. 19, No. 1, January–February 2003

Numerical Study of Cryogenic Jets Under Supercritical Conditions

J. M. M. Barata*
Universidade da Beira Interior, 6201-001 Covilhã, Portugal
I. Gökalp†
Centre National de la Recherche Scientifique, 45071 Orléans Cedex 2, France
and
A. R. R. Silva‡
Universidade da Beira Interior, 6201-001 Covilhã, Portugal

The present work is devoted to the study of cryogenic nitrogen jets in sub- and supercritical conditions. A general trend to operate under increasingly higher combustor pressures is observed in rockets, gas turbines, and diesel engines, primarily as a result of enhanced effects on thrust, power, or efficiency. In these conditions the injected fluid(s) can experience ambient pressures exceeding the critical pressure(s) of the propellants, and recent experimental work of Chehroudi et al. showed a quantitative similarity to gas-jet-like behavior (Chehroudi, B., Cohn, R., and Talley, D., "Spray/Gas Behaviour of Cryogenic Fluids under Sub- and Supercritical Conditions," Paper, July 2000; Chehroudi, B., Cohn, R., and Talley, D., "Initial Growth Rate and Visual Characteristics of a Round Jet into a Sub- to Supercritical Environment of Relevance to Rocket, Gas Turbine, and Diesel Engines," AIAA Paper 99-0206, Jan. 1999). This conclusion suggested that it would be expected that the mathematical models and numerical methods used for gaseous flows could also be used for supercritical flows. This paper reports an investigation, exploring this hypothesis, and aims to evaluate the capabilities and limitations of a computational method developed for incompressible but variable density flows when applied to supercritical conditions. The predicted initial jet growth rate was compared with available experimental data for liquid/gaseous jets and mixing layers and showed a good agreement for different supercritical density ratios. For subcritical conditions, when the flow deviates from the gaseous-like behavior, and approaches a more spray-like behavior the incompressible gaseous flow formulation was found inadequate.

Nomenclature

C_μ	=	coefficient in turbulence model
D	=	diameter of the jet
F	=	mixture fraction
k	=	turbulent kinetic energy
Pn	=	normalized pressure (pressure ratio $= p_\infty / p_{\mathrm{cr}}$)
p	=	pressure
Re	=	Reynolds number
r	=	radial coordinate
S_ϕ	=	source term
U	=	axial velocity, $U = \tilde{U} + u''$
V	=	radial velocity, $V = \tilde{V} + v''$
X	=	axial coordinate
δ	=	jet thickness
ε	=	dissipation of turbulent kinetic energy
ν_t	=	turbulent kinematic viscosity
ρ	=	density
ϕ	=	generalized variable
ω	=	density ratio (ρ_∞/ρ_0)
Γ	=	diffusion coefficient

Subscripts

cl	=	centerline values
cr	=	critical values
0	=	jet exit conditions
∞	=	chamber ambient conditions

Superscripts

$\tilde{\phi}$	=	Favre average of ϕ
$\bar{\phi}$	=	conventional average of ϕ
$''$	=	Favre fluctuation
$'$	=	conventional fluctuation

Introduction

THE present work is devoted to the study of cryogenic nitrogen jets in sub- and supercritical conditions, which has become a major domain of research with challenging fundamental aspects attracting increasing interest. A general trend to operate under increasingly higher combustor pressures is observed in rockets, gas turbines, and diesel engines, primarily as a result of enhanced effects on thrust, power, or efficiency. In these conditions the injected fluid(s) might experience ambient pressures exceeding the critical pressure(s) of the propellants. For example, in the cryogenic liquid hydrogen/liquid oxygen space shuttle main engine the thrust chamber pressure is about 22.3 MPa, whereas thrust chamber pressures for the Vulcain (Ariane 5) engine have been recorded to reach up to 10 MPa. Both of these pressures exceed the critical pressure of $P_{\mathrm{cr}} = 5.043$ MPa for liquid oxygen. In these applications the initial temperature of the oxygen can initially be below the critical temperature of the oxygen ($T_{\mathrm{cr}} = 154.58$ K) and then undergo a transition to a supercritical temperature as the oxygen is mixed and burned in the combustion chamber. The distinct difference between gas and liquid phases disappears when the pressure exceeds the critical pressure or

Received 25 January 2002; revision received 18 September 2002; accepted for publication 30 September 2002.

*Full Professor, Aerospace Sciences Department, Rua Marquês d'Ávila e Bolama. Associate Fellow AIAA.
†Research Director, Laboratoire de Combustion et Systèmes Réactifs, 1C, Avenue de la Recherche Scientifique. Senior Member AIAA.
‡Ph.D. Student, Aerospace Sciences Department, Rua Marquês d'Ávila e Bolama.

temperature exceeds the critical mixing temperature for single component fluids. Surface tension and enthalpy of vaporization vanish, and large variations in the density, thermal conductivity, and mass diffusivity occur near the critical point.[1,2] For the multicomponent fluids the solubility of the gas phase in the liquid phase increases as pressure approaches the critical pressure, and mixture effects need to be taken into account in calculating the critical properties. The critical properties of mixtures are referred to as the critical mixing temperature and the critical mixing pressure.

Some experimental and theoretical investigations[3,4] have been carried out on cryogenic jets. These studies have been concentrated on the structure of the jet under trans- and supercritical conditions and involved mainly visualization techniques. They reported a gas-jet-like visual appearance at a supercritical chamber temperature and pressure with no evidence of droplets, even when the jet was initially cool enough to be densified. More quantitative studies[5,6] have also been performed using Raman scattering, and they have shown the thermodynamic state of an injected supercritical fluid was of prime importance in determining the jet growth, not the injection velocity or momentum. These studies provide an important qualitative picture of these kinds of flows, but only recent works[1,2,6–8] have given some information adequate for modeling purposes. At supercritical pressures, not only do jets have the same appearance of a turbulent gas jet, but they have the same growth rate as incompressible variable-density turbulent jets. So, the more evident concepts and models working well for liquid sprays should fail in predicting jet flows in trans- and supercritical region. An alternative is to combine the classical Lagrangian–Eulerian (two-phase flow) approach with an Eulerian implementation to treat a multicomponent fluid (e.g., Yang[9]). The main difficulty of this "generalized" method is the representation of mixture properties that requires a microscopic analysis of the fluid. These methods would be applicable to the full range of thermophysical regimes, but their success it is still limited because of a lack a validated theories.[9]

Following the conclusions of the experimental work, the present paper reports a numerical study of cryogenic jets injected initially at subcritical temperature into an environment at a supercritical temperature over a range of subcritical and supercritical pressures and aims to evaluate the capabilities of a computational method developed for gaseous flows when applied to supercritical conditions. The approach adopted here has been applied to variable density jets, and its performance is evaluated and reported to the present case of supercritical jets.

The flow configuration is shown in Fig. 1. The cryogenic nitrogen jet (LN_2) is injected initially at subcritical temperature of 100–110 K into an environment at an ambient temperature (300 K) gaseous nitrogen (GN_2) over a range of subcritical and supercritical pressures. The exit diameter jet is 0.254 mm. The run cases are summarized in Table 1.

The normalized pressure Pn is defined to be the ratio of the chamber pressure to the critical pressure ($P_{cr} = 3.39$ MPa; $T_{cr} = 126.2$ K), and the Reynolds numbers is based on the jet exit conditions. The next section gives details of the mathematical model. The Results section presents quantitative comparison of numerical results with the measurements and theories. The final section summarizes the main findings and conclusions of this work.

Table 1 Summary of test conditions

Case	Pn	Re	T_0, k	ρ_0, kg/m^3	ρ_∞, kg/m^3	ω
1	0.91	75.281×10^3	100	702.5	34.8	0.0495
2	1.22	66.609×10^3	100	708.1	46.6	0.0658
3	2.71	42.830×10^3	100	730.8	102.9	0.1408

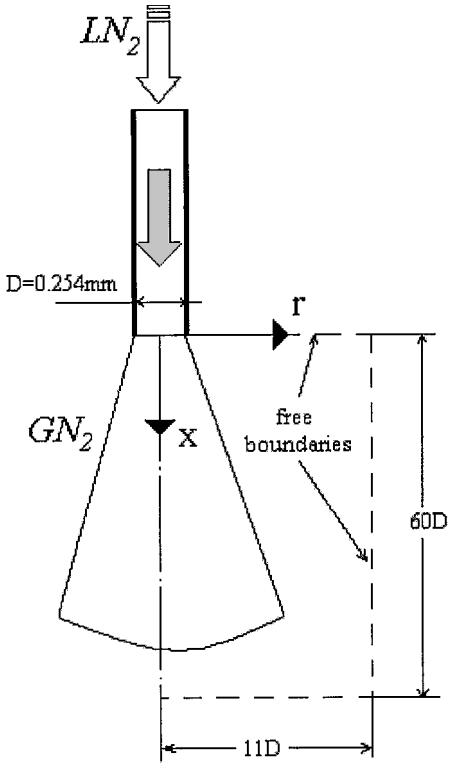

Fig. 1 Flow configuration: – – –, solution domain.

Mathematical Model

Governing Equations

The method to solve variable density jet flows is based on the solution of the conservation equations for momentum and mass. Turbulence is modeled with the k–ε turbulence model. A similar method has been used for three-dimensional[10] or axissymmetric flows,[11–13] and only the main features are summarized here.

In the conservation equations mass-weighted averaging is applied to avoid the appearance of many terms involving density fluctuations for which additional models are needed. A mass-averaged quantity is defined using Favre averaging:

$$\tilde{\phi} = \overline{\rho\phi}/\bar{\rho} \tag{1}$$

For the governing equations the standard parabolic truncation is employed. The mass-averaged partial differential equations governing the steady, variable density axisymmetric flow can be written in cylindrical polar coordinates as

$$\frac{\partial \bar{\rho}\widetilde{UU}}{\partial x} + \frac{1}{r}\frac{\partial r\bar{\rho}\widetilde{UV}}{\partial r} = -\frac{\partial \bar{p}}{\partial x} - \frac{1}{r}\frac{\partial r\bar{\rho}\widetilde{u''v''}}{\partial r} \tag{2}$$

$$\frac{\partial \bar{\rho}\widetilde{UV}}{\partial x} + \frac{1}{r}\frac{\partial r\bar{\rho}\widetilde{VV}}{\partial r} = -\frac{\partial \bar{p}}{\partial x} - \frac{1}{r}\frac{\partial r\bar{\rho}\widetilde{v''v''}}{\partial r} + \bar{\rho}\frac{\widetilde{w''w''}}{r} \tag{3}$$

and the continuity equation as

$$\frac{\partial \bar{\rho}\tilde{U}}{\partial x} + \frac{1}{r}\frac{\partial r\bar{\rho}\tilde{V}}{\partial r} = 0 \tag{4}$$

To describe mixing of gases, the mixture fraction F that represents the mass fraction of the nozzle fluid is introduced. It obeys a convection-diffusion equation of the form

$$\frac{\partial \bar{\rho}\widetilde{UF}}{\partial x} + \frac{1}{r}\frac{\partial r\bar{\rho}\widetilde{VF}}{\partial r} = -\frac{1}{r}\frac{\partial r\bar{\rho}\widetilde{u''f''}}{\partial r} \tag{5}$$

In k–ε turbulence model the Reynolds stresses are expressed in terms of the local strain rate:

$$-\bar{\rho}\widetilde{u_i''u_j''} = \bar{\rho}(\nu_t + \nu)\left(\frac{\partial \tilde{u}_i}{\partial x_j} + \frac{\partial \tilde{u}_j}{\partial x_i}\right) - \frac{2}{3}\delta_{ij}\left[\bar{\rho}k + \bar{\rho}(\nu_t + \nu)\frac{\partial \tilde{u}_j}{\partial x_j}\right] \tag{6}$$

with

$$\nu_t = C_\mu(k^2/\varepsilon) \tag{7}$$

The scalar flux in Eq. (5) is approximated with a gradient transport assumption

$$\widetilde{u_i'' f''} = -\frac{\nu_t}{\sigma_f}\frac{\partial \tilde{F}}{\partial x_i} \tag{8}$$

From the foregoing we can deduce the parabolized set of equations in cylindrical coordinates where the generalized equation is

$$\frac{\partial}{\partial x}(\bar{\rho}U\tilde{\phi}) + \frac{1}{r}\frac{\partial}{\partial r}(r\tilde{V}\bar{\rho}\tilde{\phi}) = \frac{1}{r}\frac{\partial}{\partial r}\left(r\bar{\rho}\Gamma\frac{\partial\tilde{\phi}}{dr}\right) + S_\phi \tag{9}$$

where $\tilde{\phi}$ can stand for any of the velocities, turbulent kinetic energy, dissipation, or scalar property, and S_ϕ takes on different values for each particular $\tilde{\phi}$, described in detail by Sanders et al.[11]

The mean density can be obtained from the mean mixture fraction using the equation of state. With constant pressure this leads to

$$1/\bar{\rho} = \tilde{F}/\rho_0 + (1-\tilde{F})/\rho_\infty \tag{10}$$

where density fluctuations have been neglected. This is allowed in isothermal jets because the instantaneous density, for which Eq. (10) is exact, is approximately a linear function of the instantaneous mixture fraction. For reacting flows, this is not true, and a probability density function (pdf) of the mixture fraction can be used to calculate the mean thermochemical variables such as the mean density.[11] In the present (supercritical) case and according to the hypothesis of gaseous jet-like behavior that motivated this work, we assumed that the jet vaporizes instantaneously, and the fluid in the chamber is treated as a mixture of two gaseous substances with densities equivalent to the jet exit and the initial ambient conditions. This is consistent with the present hypothesis and is supported by the experimental observations of Refs. 6 and 7, which showed no evidence of droplets and a fast change of the fluid structures at the instant of mass injection of rapidly thereafter.

Numerical Method

The governing equations are solved using a parabolized marching algorithm that resembles the (elliptic) TEACH code.[14] The computations are performed by using the continuity equation to obtain the radial velocity V. Using the radial momentum equation for V and solving a pressure correction equation for V in radial direction did not show any difference with the use of the continuity equation.[11] The approach adopted here has been applied to variable density jets, and its performance is evaluated and reported to the present case of supercritical jets. The computer code was not written for this situation, and special attention was required to avoid oscillations or divergence of the iterative process as a result of the high-density gradients. To control the numerical problems, different grids were tested, and high underrelaxation for the momentum equations was used (up to 90%).

Boundary Conditions

The computation domain has four boundaries where the boundary conditions are specified (see Fig. 1). The sensitivity of the solutions to the locations of the boundaries was investigated, and their final position is sufficiently far away from the jet so that the influence on the computed results is negligible.

The boundary that contains the jet exit is located at $X = 0$. For $0 < r < D/2$ (jet exit) a constant velocity profile based on the experimental values was used for the axial velocity, and the radial velocity is zero. The mixture fraction is one at the jet exit, which indicates the "fluid" at the instant just before the gaseous state. For $r > D/2$ a "free boundary" is prescribed by setting the pressure constant and obtaining the velocity components from continuity and momentum. This boundary condition was required to simulate the experimental conditions, but requires strong underrelaxation to avoid stability problems. The turbulent quantities were prescribed at the jet exit using a turbulence intensity of 0.1% and a length scale equal to the jet diameter and a velocity scale equal to the mean jet exit velocity. Different values of the turbulence intensity do not affect significantly the downstream flow development because a constant velocity profile at the jet exit is used (for example, see Barata[15]).

On the symmetry axis ($r = 0$) the normal velocity vanishes, and the normal derivatives of the other variables are zero.

At the outflow boundary ($X/D = 60$) the gradients of all of the dependent variables in the axial direction are set to zero. For the axial velocity component a second adjustment is done to ensure global mass conservation, which is required so that the pressure correction equation has a solution.[15]

At the boundary that is parallel to the symmetry axis and connects the inlet and outlet planes, the free boundary just mentioned is used.

Results and Discussion

The numerical predictions presented in this section are compared with measurements[1–3,16] and theories.[17–20] The main objective is to evaluate to which extent the qualitative and quantitative similarity to gas-jet-like behavior reported by Chehroudi et al.[1,2] is verified numerically when a computational method developed for gaseous variable density flows is applied to supercritical conditions.

The axial velocity decay is used to test the grid dependency of the computations. Figure 2 compares the evaluation along the axis of symmetry of the velocity decay for different grid sizes and shows that the results are already independent of numerical influences for 27×37 grids. Nevertheless, to increase the precision on the evaluation of the half-width of the jet a finer grid of 33×44 points was adopted.

Figure 3 shows typical velocity and scalar fields of the jets under subcritical and supercritical conditions. They correspond to a liquid nitrogen jet having a critical pressure of P_{cr} of 3.39 MPa at a subcritical temperature of 100 K injected into an ambient of gaseous nitrogen at a fixed supercritical temperature of 300 K and pressures of a) $0.91P_{cr}$ and b) $2.71P_{cr}$. The mixture fraction and density contours show clearly the rapid change of the jet structure near its exit ($X = 0$) for both cases, although axial variation for the supercritical conditions is even more pronounced. Furthermore, the length and thickness of the dense core decreases as the chamber pressure increases (see Fig. 4) and approaches the values observed for a pure gaseous jet. Other parameters are usually used to describe the structure of gaseous jets and shear layers such as the axial velocity decay, the widths of half-maximum of the density and velocity, and the jet growth rates (e.g., Abramovich[17]). These parameters show in general a linear variation with the axial distance when the flow becomes fully turbulent and the radial profiles of the axial velocity become similar 8 to 12 diameters downstream of the jet exit. In the next

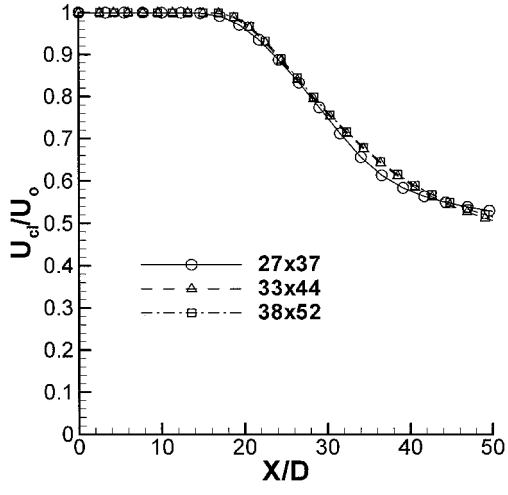

Fig. 2 Grid size dependency test based on the axial velocity decay.

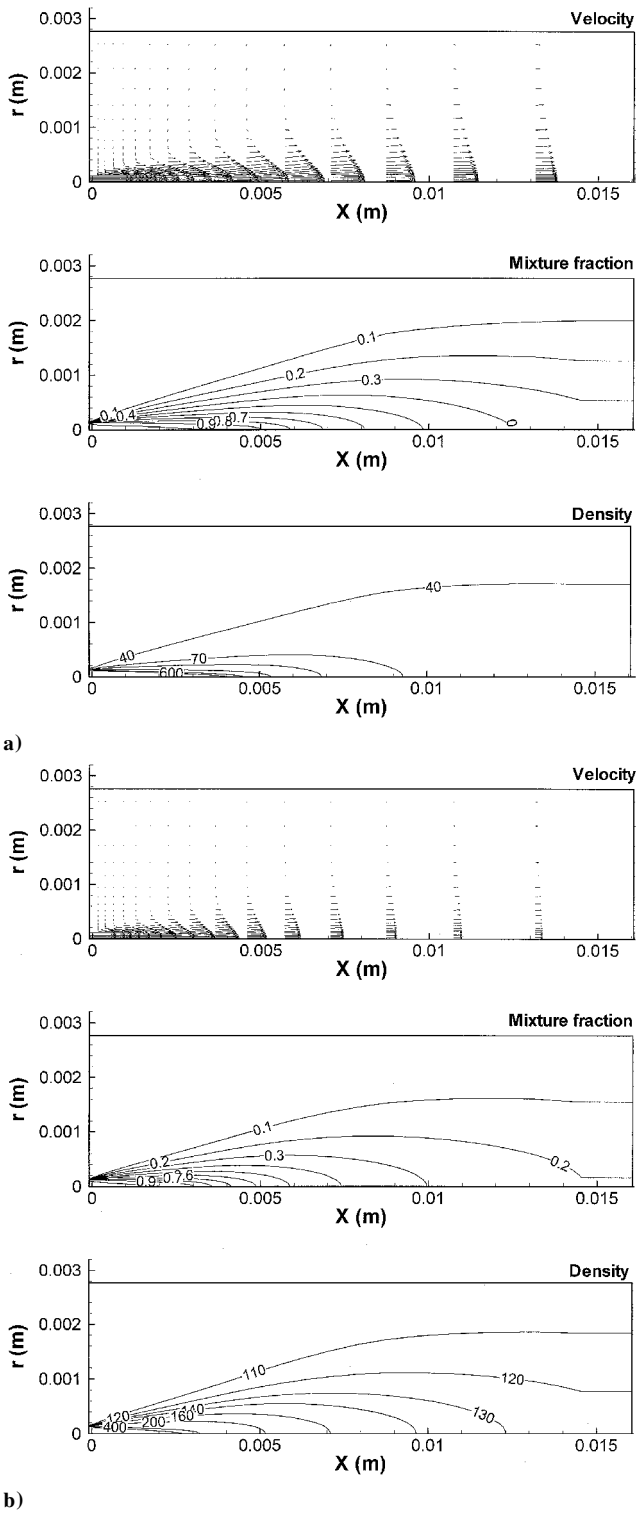

Fig. 3 Velocity and scalar fields of the jets under a) subcritical ($Pn = 0.91$) and b) supercritical conditions ($Pn = 2.71$).

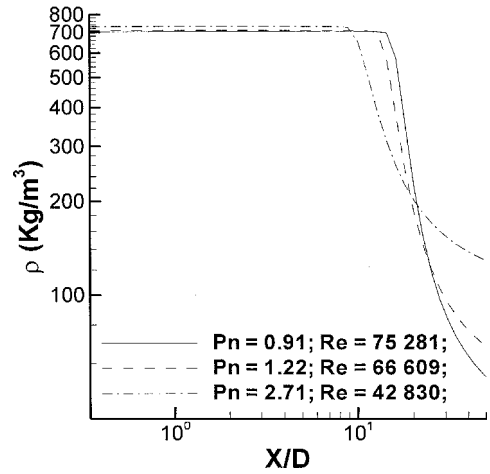

Fig. 4 Axial variation of centerline density.

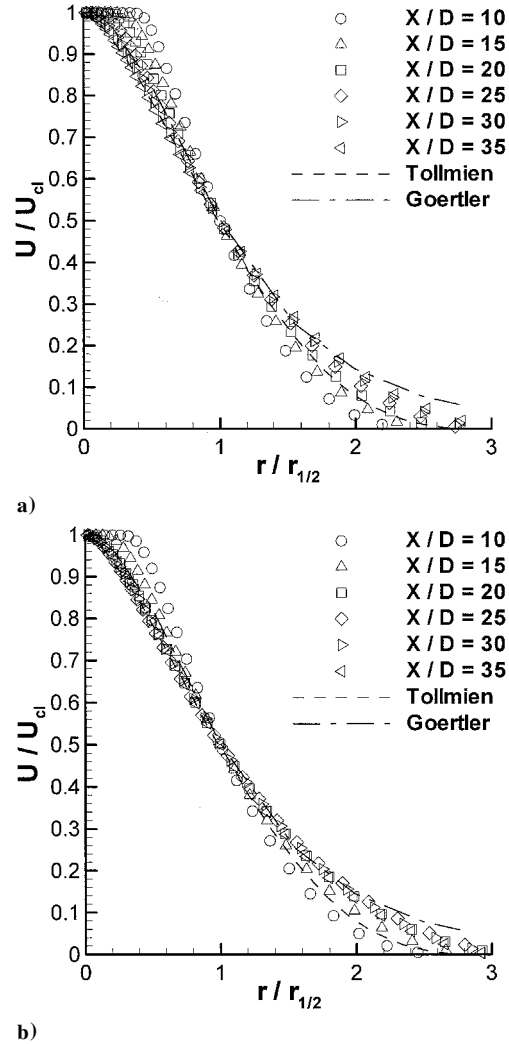

Fig. 5 Nondimensional profiles of the mean axial velocity: a) $Pn = 0.91$, subcritical; b) $Pn = 2.71$, supercritical.

paragraphs these type of parameters are used to analyze the linear growth of the subcritical and supercritical jets. To allow comparison with the experiments, all of the jet growth rates are converted to "visual" growth rates using the ratio between the measured and visual thickness proposed by Papamoschou and Roshko.[19]

Figure 5 compares the nondimensionalized axial velocity profiles for a) subcritical and b) supercritical conditions. The analytical solutions of Tollmien and Goertler (see Ref. 18 for details) for turbulent axisymmetric free jets are also represented in the figure. The analysis of a large number of experimental data have shown that near the axis ($r/r_{1/2} < 1$) the Goertler curve is slightly superior to the Tollmien curve, whereas in the outer regions ($r/r_{1/2} > 1$) the Tollmien curve agrees with the measurements much better than the Goertler-type curve. This behavior can also be observed in Fig. 5a for the subcritical conditions ($Pn = 0.91$) for $X/D > 20$. For supercritical conditions ($Pn = 2.71$) the nondimensional axial velocity profiles are coincident with the Goertler curve near the axis for $X/D > 15$, and in the outer region they are also closer to this curve

(Fig. 5b). Figure 6 shows the axial velocity decay along the centerline. The curves exhibit a linear portion that begins closer to the jet exit when the normalized pressure increases. This is in agreement with the similar velocity profiles presented in Fig. 5. For $Pn = 0.91$ (Fig. 5a) the velocity profiles become similar for $X/D > 20$, whereas for $Pn = 2.71$ (Fig. 5b) they are already similar for $X/D > 15$. The results also show that the velocity decay along the centerline increases when the normalized pressure increases but with a smaller rate than the Goertler or Tollmien curves. This result indicates that the computational jet growth rates cannot be obtained from the axial velocity decay as in an isothermal turbulent jet. A similar conclusion is presented by Oschwald et al.[5] from experimental data. These authors have shown that the thermodynamic state of an injected supercritical fluid was of prime importance in determining the jet growth rate and not the velocity or momentum. In fact, the more significant changes occur in the shear layer surrounding the jet where the largest gradients of density exist. It could then be inferred that only the jet spreading calculated from the density half-widths would give representative values, but, actually, as shown in Fig. 7, the full width of half-maximum of the velocity agrees quite well with Tollmien and Goertler curves for gaseous jets and confirms the similarity of the velocity profiles already mentioned. Furthermore, a completely different result is obtained using the full width of half-maximum of the density profile, and no linear variation can be clearly identified. The reduction of the potential core already mentioned before is associated with an enhanced mixing between the jet and the surrounding fluid near the jet exit. As a consequence, the jet growth can be noted for a smaller axial distance. In this region a major deviation from the gas-like behavior can be inferred by the full width at half-maximum of the density, which decays instead of assuming a constant value of $D_{1/2}/D = 1$ (e.g., Abramovich[17]).

In Fig. 8 the jet width defined and related to the visual shear-layer thickness by Papamoschou and Roshko[19] is represented. The jet growth rates can be obtained from this figure by calculating the tangent of the divergence angle and are plotted in Fig. 9. This figure

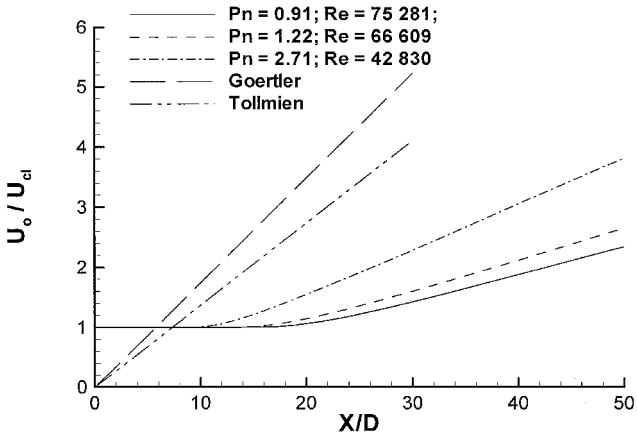

Fig. 6 Centerline velocity decay.

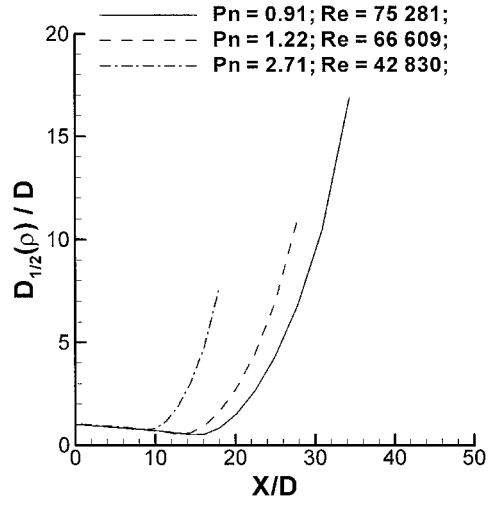

a)

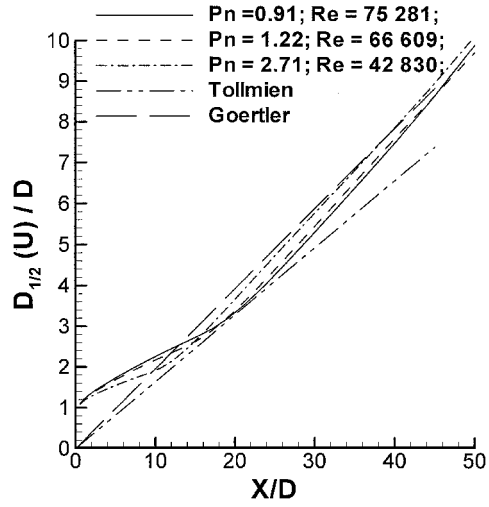

b)

Fig. 7 Full width of half-maximum of the a) density and b) velocity.

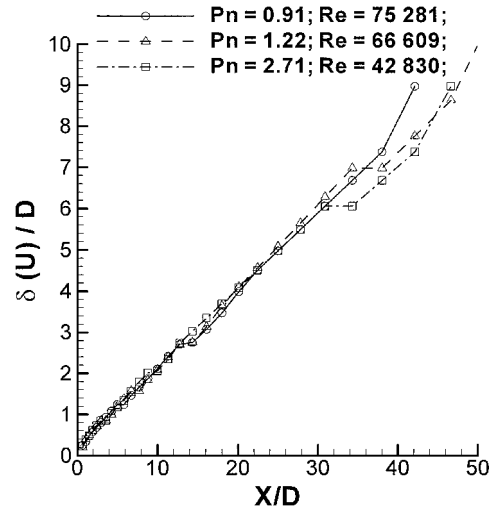

Fig. 8 Jet width growth along the centerline.

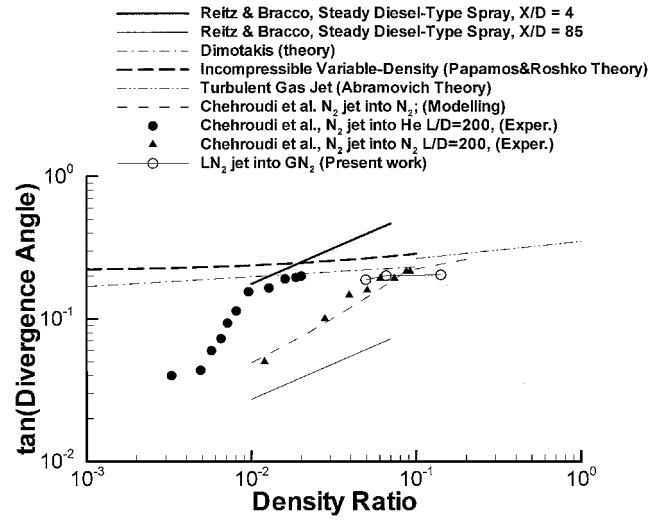

Fig. 9 Tangent of the spreading angle vs chamber-to-injectant density ratio.

shows the influence of the chamber-to-injectant density ratio into jet spray or mixing layer divergence angle. At density ratios large enough to correspond to supercritical chamber pressures, when the jet appearance was found to visually resemble that of a turbulent gas jet, the predictions are in agreement with the equation proposed by Chehroudi et al.[1] and closely follow the tendency of the theoretical equations proposed by Dimotakis[20] and Papamoschou and Roshko,[19] both for incompressible variable density layers. As the density ratio was decreased, the growth rate also decreases. At a certain density ratio corresponding to chamber pressure near the critical pressure, the predictions are still in agreement with the preceding equations and measurements.[1,6] As expected, if the density ratio is further decreased below the transition value some disagreement with the experimental data of the Chehroudi et al.[1,2] and Woodward and Talley[6] will be observed because the jets approach the spray behavior.

Conclusions

A computational program developed for gaseous and variable density flows was used to study cryogenic jets injected initially at a subcritical temperature into an environment at a supercritical temperature over a range of subcritical and supercritical pressures. The aim was to evaluate its suitability to predict this type of flow. The cryogenic nitrogen jet was injected initially at subcritical temperature of 100–110 K into an environment at ambient temperature gaseous nitrogen over a range of subcritical and supercritical pressures. The approach adopted here has been applied to variable density jets, and its performance was evaluated and reported for the present case of supercritical jets. The computational code was not written for this situation, but has behaved quite well, confirming the hypothesis that a supercritical flow that looks like a gaseous flow can be calculated like a gaseous flow. The predictions were compared with measurements and theories and in general show a good agreement. The jets have quantitatively the same growth rates as incompressible variable density turbulent jets but at supercritical pressures. For subcritical conditions, when the flow deviates from the gaseous-like behavior and approaches a more spray-like behavior, the incompressible gaseous formulation was found inadequate.

The computer program revealed great capabilities to study cryogenic jets injected initially at a subcritical temperature into an environment at a supercritical temperature over a range of subcritical and supercritical pressures, but different numerical solving models should be developed to integrate also the two-phase flow regime.

Acknowledgments

The present work has been performed in the scope of the activities of the AeroThermodynamics Group for Aerospace Sciences and Technology and Laboratory the Combustion and Reactive Systems. The financial support of the ICCTI of the Portuguese Ministry of Science and the French Embassy under Contract 415 B4 and Grant 280415H is gratefully acknowledged.

References

[1]Chehroudi, B., Cohn, R., and Talley, D., "Spray/Gas Behaviour of Cryogenic Fluids Under Sub- and Supercritical Conditions," *Eighth International Conference on Liquid Atomization and Sprays Systems*, ICLASS, July 2000.

[2]Chehroudi, B., Cohn, R., and Talley, D., "Initial Growth Rate and Visual Characteristics of a Round Jet into a Sub- to Supercritical Environment of Relevance to Rocket, Gas Turbine, and Diesel Engines," AIAA Paper 99-0206, Jan. 1999.

[3]Mayer, W., and Tamura, H., "Propellant Injection in a Liquid Oxygen/Gaseous Hydrogen Rocket Engine," *Journal of Propulsion and Power*, Vol. 12, No. 6, 1996, pp. 1137–1147.

[4]Mayer, W. O. H., Schick, A. H. A., Vielle, B., Chauveau, C., Gökalp, I., Talley, D. G., and Woodward, R. D., "Atomization and Breakup of Cryogenic Propellants Under High-Pressure Subcritical and Supercritical Conditions," *Journal of Propulsion and Power*, Vol. 14, No. 5, 1998, pp. 835–842.

[5]Oschwald, M., Schik, A., and Mayer, W., "Investigation of Coaxial LN2/GH2-Injection at Supercritical Pressure by Spontaneous Raman Scattering," AIAA Paper 99-2887, June 1999.

[6]Woodward, R. D., and Talley, D. G., "Raman Imaging of Transcritical Cryogenic Propellants," AIAA Paper 96-0468, 1996.

[7]Chehroudi, B., Cohn, R., and Talley, D., "Cryogenic Shear Layers: Experiments and Phenomenological Modeling of the Initial Growth Rate Under Subcritical and Supercritical Conditions," *International Journal of Heat and Fluid Flow*, Vol. 23, 2002, pp. 554–563.

[8]Chehroudi, B., Talley, D., and Coy, E., "Anatomical Changes of a Cryogenic Jet in Transition to Thermodynamic Supercritical Condition," ILASS-Europe'99, July 1998.

[9]Yang, V., "Modeling of Supercritical Vaporization, Mixing, and Combustion Processes in Liquid-Fueled Propulsion Systems," *Proceedings of the Combustion Institute*, Vol. 28, 2000, pp. 925–942.

[10]Barata, J. M. M., "Numerical Study of Single Impinging Jets Through a Crossflow," *Journal of Aircraft*, Vol. 26, No. 11, 1989, pp. 1002–1008.

[11]Sanders, J. P. H., Sarh, B., and Gökalp, I., "Variable Density Effects in Axisymmetric Isothermal Turbulent Jets: a Comparison Between a First- and a Second-Order Turbulence Model," *International Journal of Heat and Mass Transfer*, Vol. 40, No. 4, 1997, pp. 823–842.

[12]Barata, J. M. M., and Perestrelo, N. F. F., "Numerical Simulation of Injection Systems for Lean Burn, Premixed, Prevaporised Combustors," XIVth International Symposium on Air Breathing Engines, ISOABE, Sept. 1999.

[13]Barata, J., and Silva, A., "Numerical Study of Spray Dispersion in a Premixing Chamber for Low-NOx Engines," *Journal of Thermal Science*, Vol. 9, No. 3, 2000, pp. 282–288.

[14]Gosman, A. D., and Pun, W. M., "Calculation of Recirculating Flows," Lecture Notes Engineering Rept. HTS 73/2, Imperial College Mech., London, 1973.

[15]Barata, J. M. M., "Estudo Numérico e Experimental de Jactos Incidentes Sobre uma Superfície Plana Através de um Escoamento Cruzado," Ph.D. Dissertation, Inst. Superior Técnico, Technical Univ. of Lisbon, Portugal, June 1989 (in Portuguese).

[16]Reitz, R. D., and Bracco, F. V., "On the Dependence of Spray Angle and Other Spray Parameters on Nozzle Design and Operating Condition," Society of Automotive Engineers, Paper 790494, Feb.–March 1979.

[17]Abramovich, G. N., *The Theory of Turbulent Jets*, MIT Press, Cambridge, MA, 1963.

[18]Rajaratnam, N., *Turbulent Jets*, Developments in Water Science, 5, Elsevier Scientific Publishing Co., New York, 1976.

[19]Papamoschou, D., and Roshko, A., "The Compressible Turbulent Shear Layer: an Experimental Study," *Journal of Fluid Mechanics*, Vol. 197, 1988, pp. 453–477.

[20]Dimotakis, P. E., "Two-Dimensional Shear-Layer Entrainment," *AIAA Journal*, Vol. 21, No. 11, 1986, pp. 1791–1796.